Astrophys Space Sci (2019) 364:146
https://doi.org/10.1007/s10509-019-3635-8

ORIGINAL ARTICLE

Abnormal magnetospheric magnetic gradient direction reverse around the indented magnetopause

Xiaojian Song[1,2,3] · **Pingbing Zuo**[3] · **Xueshang Feng**[1] · **Jih-Hong Shue**[4] · **Yi Wang**[3] · **Chaowei Jiang**[3] · **Zilu Zhou**[1,2,3] · **Xiaojun Xu**[5]

Received: 13 June 2019 / Accepted: 27 August 2019

Abstract Time History of Events and Macroscale Interactions during Substorms (THEMIS) data are used to investigate the magnetic field structures in the vicinity of the magnetopause. Generally, the tendency that the farther away from the Earth, the weaker the detected magnetic field is expected inside the dayside magnetopause. Here we show two cases which conflict with the expectation that the magnetic field gradient direction reverses from inward to outward in a short time interval. After a further analysis, it is found that the THEMIS probes encountered a magnetopause indentation moving along the magnetopause towards the dawn in one case, and for the other case, they crossed an evolutive indented magnetopause that was produced locally and then recovered to its normal state. These two magnetopause indentation may be related with the fast magnetosheath flow. Accordingly, we suppose that the fast magnetic gradient direction reverse is caused by the abnormal magnetic field distribution adjacent to the deformed magnetopause.

Keywords Magnetopause indentation · Reversed magnetic gradient · Data analysis

✉ P. Zuo
pbzuo@hit.edu.cn

1 SIGMA Weather Group, State Key Laboratory for Space Weather, National Space Science Center, Chinese Academy of Sciences, Beijing 100190, China

2 University of Chinese Academy of Sciences, Beijing 100190, China

3 Laboratory for Space Weather Storms, Institute of Space Science and Applied Technology, Harbin Institute of Technology, Shenzhen, Shenzhen 518055, China

4 Institute of Space Science, National Central University, Taoyuan, Taiwan

5 State Key Laboratory of Lunar and Planetary Sciences, Macau University of Science and Technology, Macao, China

1 Introduction

The magnetopause is the interface between the magnetosphere which consists of tenuous high energy plasma and strong magnetic fields originated from the Earth, and the magnetosheath which fills with dense low energy plasma and weaker magnetic fields originated from the Sun. The location and shape of the magnetopause are determined by the total pressure (the sum of dynamic pressure, thermal pressure and magnetic pressure) balances between the magnetosphere and the magnetosheath (Spreiter et al. 1966). When the dynamic pressure of the solar wind (SW) is enhanced, the total pressure in the magnetosheath increases and the magnetopause is pushed closer to the Earth, which results in the magnetic field compression and enhancement of the magnetic pressure in the magnetosphere. The total pressure on both sides of the magnetopause reaches equilibrium again at a later time.

There are lots of models to describe the location and shape of the magnetopause (e.g., Fairfield 1971; Petrinec et al. 1991; Shue et al. 1998; Song et al. 1999). They are all based on statistical results of observations of magnetopause crossings. The fitted shape of the magnetopause assumed in the models is a smooth surface. However, the magnetopause surface waves can arise or grow due to the boundary-inherent Kelvin-Helmholtz-instability (KHI), or be generated by external sources, e.g., SW pressure pulses or waves and disturbances originating in the foreshock region (e.g., Fairfield et al. 1990; Fujita et al. 1996; Glassmeier and Heppner 1992; Plaschke et al. 2013). Local distortions of the magnetopause may be driven by flux transfer events, Kelvin-Helmholtz waves, and the magnetosheath pressure pulses related to magnetic reconnections, flow shears, hot flow anomalies, foreshock cavities, and transient density events, etc. (Dmitriev and Suvorova 2012). All of these

Published online: 05 September 2019

make the magnetopause no longer a smooth surface. In fact in the literature, some events of magnetopause indentation due to the local distortion have been depicted from multiple spacecrafts data analysis. Shue et al. (2009) reported an local indentation on the magnetopause, 1 R_E deep and 2 R_E wide, and proved that it resulted from an increase of the solar wind velocity in the magnetosheath, associated with the radial magnetic field in the solar wind. Tkachenko et al. (2011) reported a series of magnetopause indentation structures moving to the dawn flank, and inferred that they may be caused by changes of the orientation of the magnetic field and by enhancements and decreases of the plasma density in the magnetosheath.

Recent studies inferred that the magnetopause indentation plays an important role in magnetosphere-ionosphere coupling (Han et al. 2016, 2018). A particular auroral form observed around dayside ionospheric convection throat region, called throat aurora (Han et al. 2015), has been suggested to be the ground signature of magnetopause indentations (Han et al. 2016, 2018). It has been confirmed that the occurrence rate of throat aurora is rather high (Han et al. 2017), which implies that the indentation often occurs at the magnetopause. Han et al. (2019) provided observational evidence for showing the throat aurora being associated with magnetopause reconnection, and thus, Han (2019) proposed a model and suggested that the magnetopause indentations are most likely caused by magnetopause reconnection. These studies using ground-based optical observations have suggested that magnetopause indentations are commonly exist. Further investigation should be made to provide more evidences from satellite observations.

The magnetic fields in the magnetosphere consist of the Earth's main magnetic field and the magnetic fields created by the current system, e.g., ring current, tail current, Chapman-Ferraro magnetopause current and so on (Chapman and Ferraro 1930; Ganushkina et al. 2015). The magnetic field just inside the magnetopause is most susceptible to the shape and location of the magnetopause. In a stable and uniform solar wind, the magnetopause is often be regarded as a smooth surface. In this case, the dayside magnetospheric magnetic field gradient points inward. It can be simulated by the magnetospheric magnetic field model (Tsyganenko 1989, 1996), and was verified by observations with multiple spacecrafts. So far, the magnetic field distribution near the indented magnetopause has not been intensively investigated. Here we report two magnetopause crossing events, which are identified to be associated with magnetopause indentations. For these two events, the dayside magnetospheric magnetic gradient direction reversed from inward to outward in a short time interval, we call it fast magnetic gradient direction reverse (FMGDR). The detailed analysis for the two events is described in Sect. 2 and discussed in Sect. 3. In Sect. 4, a brief summary is given.

2 Indented magnetopause crossings

The THEMIS fleet was launched into a near-equatorial, highly elliptical orbit on 17 February 2007 (Angelopoulos 2008). The five THEMIS probes were lined up in the same orbit like a string of pearls before a modification of their orbits was performed at the end of 2007. Each of the THEMIS probes carries an identical instrumentation including a fluxgate magnetometer (FGM), an electrostatic analyser (ESA), a solid state telescope (SST), a search coil magnetometer (SCM) and an electric field instrument (EFI). In this paper, the magnetic field measurements from FGM (Auster et al. 2008) and plasma measurements provided by ESA (McFadden et al. 2008) with time resolution of ~ 3 s are used.

2.1 Event 1: 00:44 UT-00:56 UT on 22 July 2007

Between 00:44 UT and 00:56 UT on 22 July 2007, the THEMIS fleet was moving outbound near the subsolar point as shown in the left panel of Fig. 1. The THEMIS probes are represented by squares with different colors. The arrows represent the velocity with the length denoting the relative speed of each probe, and the red arc is the magnetopause calculated by the Shue et al. (1998) model. Since the time period was very short and the velocity ($\sim$1 km/s) of probes were small, we consider that the probes were fixed at each point. THB was located at $(11.44, -2.16, -3.10)$ R_E, THC was located at $(10.92, -2.41, -2.94)$ R_E, THD was located at $(10.92, -2.45, -2.92)$ R_E, THE was located at $(10.74, -2.40, -2.91)$ R_E and THA was located at $(9.27, -3.10, -2.39)$ R_E. THB was leading on this outbound pass and followed by THC, THD, THE and THA in sequence. THC and THD were very close to each other (here we treat them as one satellite THC&D) and the distance between THA and THB was about 2 R_E.

The right panel of Fig. 1 shows the interplanetary condition observed by WIND during this time interval. The observations are simply shifted based on the location of WIND and the velocity of solar wind ($dt = (X_{WIND} - R_0)/V_x$, dt is the time used to shift, X_{WIND} is the X component of the location of WIND, R_0 is the location of the magnetopause nose, V_x is the X component of solar wind velocity). The parameters from top to bottom are: three components of interplanetary magnetic field (IMF), cone angle of IMF, velocity of the solar wind, solar wind number density. The analyzed time interval is bounded by two vertical dashed lines. It can be seen that there was no clear pressure pulse. At the beginning of this time interval, the cone angle of IMF was small and it kept increasing to a big value at the end of the time interval.

The ion spectral energy flux density and ion bulk velocity measurements between 00:44 UT and 00:56 UT are shown in Fig. 2. It can be seen that four (THB, THC, THD, THE)

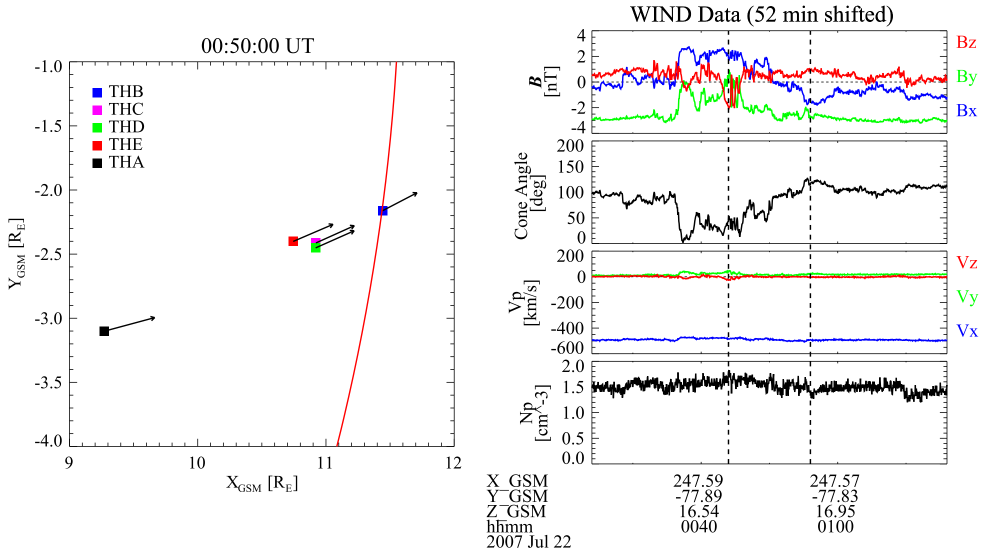

Fig. 1 (left): The projection of the locations of five THEMIS probes on the X–Y plane at 00:50:00 UT on 22 July 2007. THEMIS probes are marked by differently colored squares. The red curve denotes the magnetopause calculated by the Shue et al. (1998) model. The black arrows show the movement direction of probes. (right): The solar wind parameters observed by WIND. From top to bottom: three components of IMF, IMF cone angle, solar wind velocity, number density of solar wind. The analyzed time interval is bounded by two vertical dashed lines

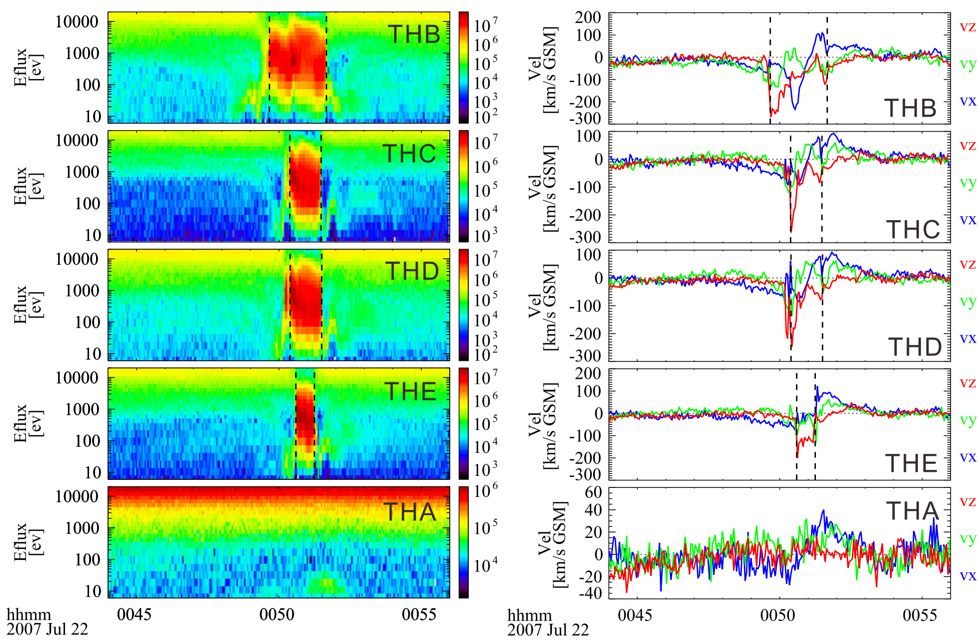

Fig. 2 The left and right panels are the ion spectral energy flux density and ion bulk velocity measurements in the GSM coordinate system from the THEMIS fleet between 00:44 UT and 00:56 UT on 22 July 2007, respectively. The magnetopause crossing times are marked by the vertical dashed lines

of the five THEMIS probes crossed the magnetopause twice during this interval. At the very beginning, the THEMIS fleet was in the magnetosphere where the high energy ions and strong magnetic fields are dominated. At 00:49:40 UT, the outermost probe, THB, crossed the magnetopause first. Then THD, THC and THE crossed the magnetopause in sequence within less than 1 minute. Between 00:50:36 UT and 00:51:14 UT, all the spacecrafts of the THEMIS fleet (except THA) were located in the magnetosheath. At 00:51:14 UT, THE returned to the magnetosphere first. Then THC, THD and THB crossed the magnetopause immediately after THE in sequence. The two crossing times for each probe are marked by the two vertical dashed lines in each subfigure. The outermost probe, THB, stayed in the magnetosheath for the longest time. The innermost probe, THA, was always located in the magnetosphere with no magnetopause crossing during the analyzed interval. The right panel of Fig. 2 shows that THB observed a rather fast anti-sunward flow in the magnetosheath at 00:50:21 UT. It increased up to 250 km/s at 00:50:36 UT and disappeared before THE crossed the magnetopause at the second time.

For comparison, we put the magnetic field strength curves for all probes during the same interval together in Fig. 3. At 00:44 UT, the order of the magnetic field strength from small to large was THB, THC&D, THE, THA (the strength observed by THB was 25% lower than that observed by THA). It means the magnetic gradient pointed inward normally. Subsequently, the magnetic field strength began to increase with different growth rates, which caused the intersections of the magnetic field strength curves. After the intersection of the curves of THB and THC&D&E (see the yellow area in Fig. 3), the magnetic field at the location of THB exceeded that at the location of THC&D&E. It means that the magnetic gradient between THB and THC&D&E changed direction and pointed outward. When the curves of THC&D&E and THA intersected with each other, the magnetic gradient between the location of them also reversed the direction. The variation of the magnetic field strength in the inbound (THEMIS fleet crossed the magnetopause to the magnetosphere) magnetopause crossing was somewhat like the mirror image of the outbound crossing, except that the magnetic field strength was overall a little smaller than that observed at the first crossing. Likewise there were intersections between different magnetic filed curves. Each intersection means that the magnetic field gradient between the two probes reversed.

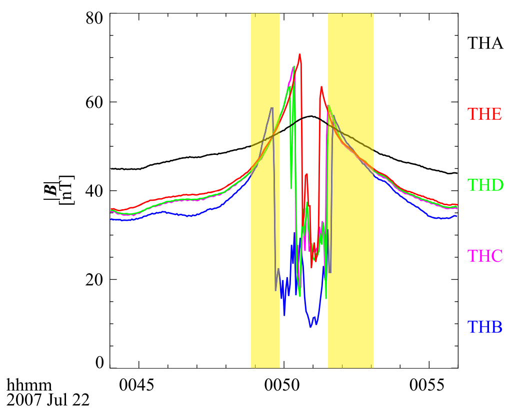

Fig. 3 The magnetic field strength observed by THEMIS fleet between 00:44 UT and 00:56 UT on 22 July 2007. The discussed FMGDRs are marked by yellow bars

To understand the structure of the magnetopause during the analyzed interval, the minimum variance analysis (MVA) method (Sonnerup and Scheible 1998) is applied to calculate the normal of the magnetopause tangential plane at the time when a magnetopause crossing was recorded. The normals calculated using the MVA method and using the referred magnetopause model (Shue et al. 1998) are compared (see Table 1). It can be seen that the change of the magnetopause normal in azimuth angle (X–Y plane) is bigger than that in the elevation angle (X–Z plane). Figure 4 shows the determined tangential planes of all the magnetopause crossings each probe encountered (short colored lines), the nominal magnetopause plane (large red arc) and the observed plasma flow vectors (black arrows) projected on to the X–Y plane. Figures 4a–d present the snapshots during which the four probes THB, THD, THC, THE crossed the magnetopause for the first time in sequence, and Figs. 4e–h correspond to their second magnetopause crossings. The exact crossing time is marked on the title of each panel. In Fig. 4a, THB crossed the magnetopause for the first time and observed an inward bulk velocity of ions. Likewise,

Table 1 The comparison of the local magnetopause normals calculated by MVA method and Shue et al. (1998) magnetopause model

	Time hh:mm:ss	Probe	Direction	Normal (MVA method)	Normal (Magnetopause model)	Angle (θ, φ)
Event 1	00:49:40	THB	Outbound	(0.97, 0.17, 0.17)	(0.97, −0.13, −0.18)	(20.4, 17.5)
	00:50:21	THD		(0.98, 0.14, 0.14)		(18.7, 15.6)
	00:50:22	THC		(0.98, 0.15, 0.13)		(18.1, 16.2)
	00:50:36	THE		(0.90, −0.35, 0.25)		(25.1, −13.7)
	00:51:14	THE	Inbound	(0.70, −0.70, 0.13)		(18.1, −37.5)
	00:51:28	THC		(0.85, −0.48, −0.20)		(−0.9, −22.0)
	00:51:30	THD		(0.82, −0.56, −0.08)		(6.0, −26.8)
	00:51:40	THB		(0.58, −0.79, 0.17)		(20.5, −46.2)
Event 2	22:24:34	THB	Outbound	(0.44, −0.86, −0.24)	(0.92, −0.35, −0.15)	(−5.0, −41.6)
	22:24:59	THC		(0.73, −0.62, −0.28)		(−7.3, −19.0)
	22:25:01	THD		(0.48, −0.82, −0.30)		(−8.6, −38.3)
	22:25:03	THE		(0.17, −0.97, −0.19)		(−2.0, −58.7)
	22:27:22	THE	Inbound	(0.49, −0.82, −0.29)		(−8.0, −37.8)
	22:28:41	THD		(0.74, −0.67, −0.02)		(7.7, −20.8)
	22:28:45	THC		(0.87, −0.50, 0.01)		(9.5, −8.5)
	22:32:18	THB		(0.82, −0.56, −0.02)		(7.8, −13.0)

Note—(θ, φ) indicate the elevation and azimuth angle between the normals calculated by MVA method and Shue et al. (1998) magnetopause model

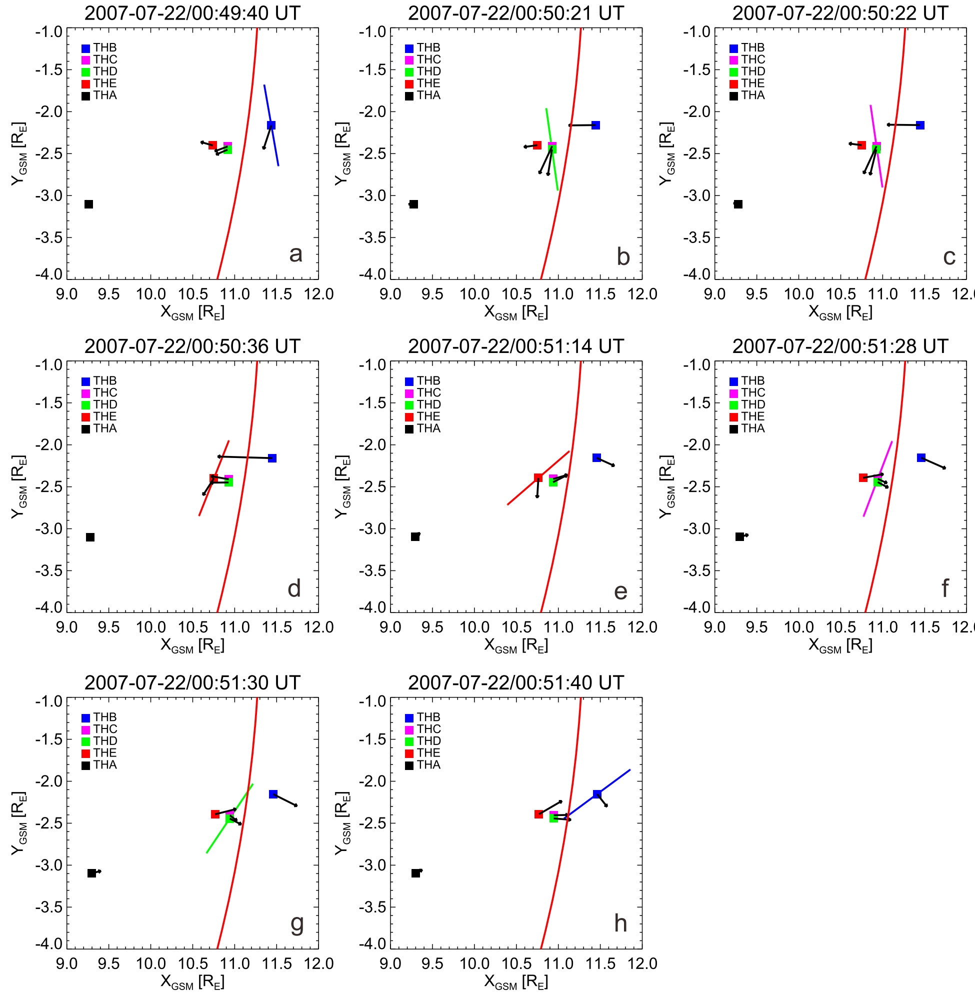

Fig. 4 Comparisons of the tangential planes calculated by MVA (short colored lines) and nominal magnetopause planes calculated by Shue et al. (1998) (large red curves). The black arrows are the plasma velocity observed by the THEMIS fleet

when THC and THD first crossed the magnetopause, they encountered the same inward motion plasma (see Figs. 4b and 4c respectively). At the same time, the anti-sunward velocity of ions in the magnetosheath was enhanced, which should be the reason for the inward motion of the magnetopause. Figure 4d corresponds to the situation for the time when THE crossed the magnetopause for the first time. The magnetopause tangential plane continued moving inward and the bulk velocity of ions was also inward because the anti-sunward velocity of ions observed by THB in the magnetosheath was the largest at this time. Note that the orientation of the magnetopause plane observed by THE had a drastic change compared to those observed by THC and THD, which can be explained by a moving indentation. As shown in Figs. 4e–h, when THE, THC, THD and THB crossed the magnetopause at the second time, the tangential plane they crossed changed a direction relative to those for the first crossing and the bulk velocity of ions became outward. On the other hand, the anti-sunward velocity of ions in the magnetosheath disappeared at the second crossing of the THEMIS fleet. The magnetopause started moving outward to its nominal position.

According to the information shown in Fig. 4, the THEMIS fleet may encounter an indentation moving along the magnetopause towards the dawn and developing deeper due to the influence of the fast anti-sunward ion flow in the magnetosheath. The sketch picture is shown in Fig. 5 with the gray area standing for the magnetosphere and the blank area standing for the magnetosheath. At 00:49:40 UT, THB crossed the leading edge of the local magnetopause indentation (see Fig. 5a). On the other hand, as the indentation was moving to the dawn, the ions observed by THB should have an inward velocity relative to the tangential plane. Likewise when the leading edge of the indentation moved to the location of THC&D, it observed an inward velocity (see Fig. 5b). At this time, the anti-sunward velocity of ions observed by THB was enhanced, it compressed and pushed the indentation to a deeper location. Subsequently, the trailing edge of the indentation crossed the probe THE (see Fig. 5c). After 00:50:36 UT, the anti-sunward ion flow began to decrease and disappeared at 00:51:14 UT, the indentation contracted

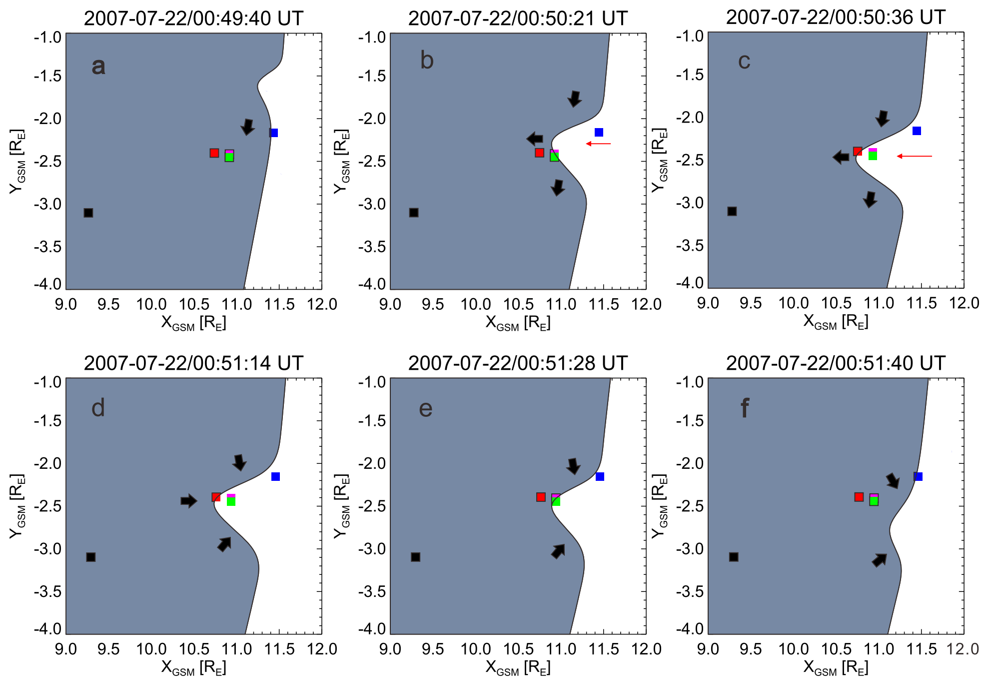

Fig. 5 Schematic pictures of the indented magnetopause. The THEMIS probes are represented by differently colored squares. The gray area is the magnetosphere. The blank area is the magnetosheath. The red arrows are the bulk velocity of ions measured in the magnetosheath with the length denoting the relative speed of ions. The black arrows represent the directions in which the magnetopause is moving

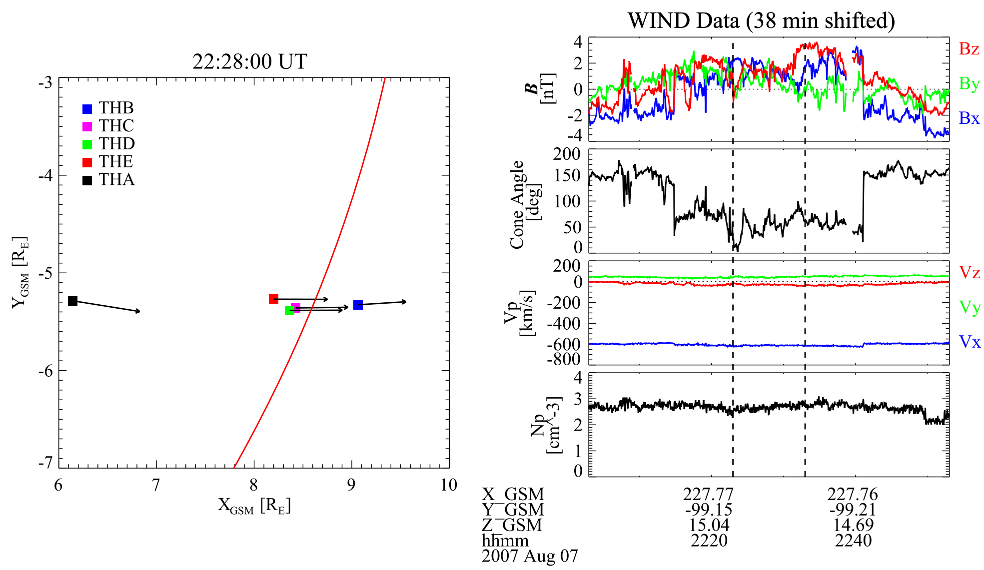

Fig. 6 (left): The projection of the locations of five THEMIS probes on the X–Y plane at 22:28:00 UT on 07 August 2007. (right): The solar wind parameters observed by WIND. The format is the same as in Fig. 1

and its trailing edge encountered THE for the second time (as shown in Fig. 5d). In the rest of the time, the indentation continued to move toward the dawn and rebounce. The trailing edge of the indentation encountered THC&D and the THB, as shown in Figs. 5e and 5f. The observed ions moved outward relative to the tangential plane. According to the above analysis, it is expected that the probes (except THE) observed a left-leaned discontinuity and then became right-leaned relative to the nominal magnetopause plane, and the ion first moved inward and then outward in pace with the twice magnetopause crossings due to the motion of the deformed local magnetopause, i.e., the indentation. This picture is well consistent with the observations presented in Fig. 4.

2.2 Event 2: 22:23 UT-22:33 UT on 07 August 2007

Between 22:23 UT and 22:33 UT on 07 August 2007, the THEMIS fleet was moving outbound near 10:00 LT, as shown in the left panel of Fig. 6. During this short time interval, THB was located at $(6.14, -5.28, -1.45)$ R_E, THC was located at $(9.06, -5.33, -2.30)$ R_E, THD was located at $(8.42, -5.36, -2.12)$ R_E, THE was located at $(8.36, -5.38, -2.09)$ R_E, THA was located at

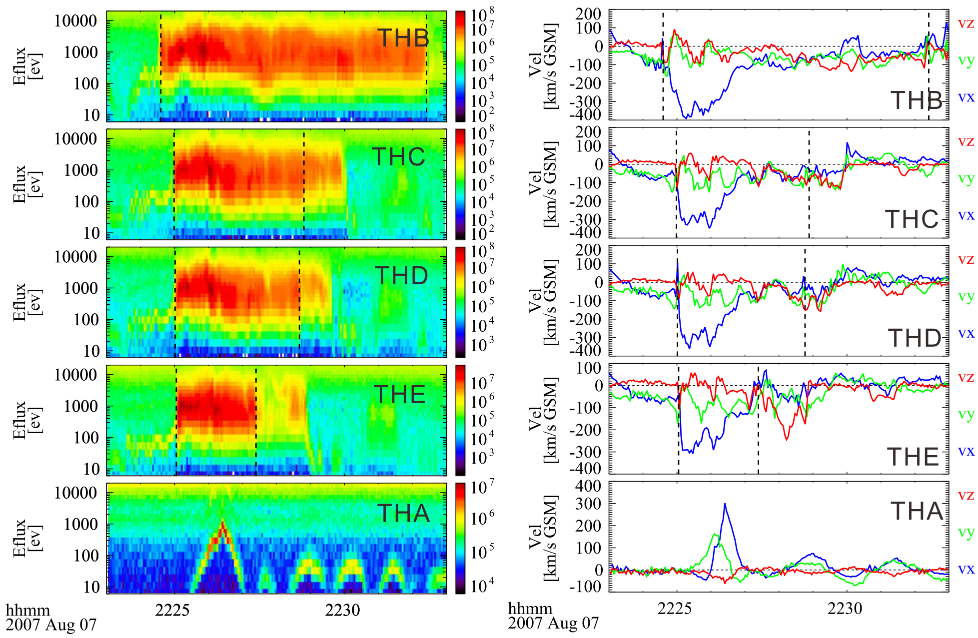

Fig. 7 The left and right panels are the ion spectral energy flux density and ion bulk velocity measurements in the GSM coordinate system from the THEMIS fleet between 22:23 UT and 22:33 UT on 07 August 2007, respectively. The magnetopause crossing times are marked by the vertical dashed lines

$(8.20, -5.27, -2.08)\ R_E$. The configuration of the THEMIS fleet was the same as that for Event 1: THB was the outermost probe, followed by THC, THD and THE, and THA was the innermost probe. The distance between THA and THB was about 3 R_E. The right panel of Fig. 6 shows that there was no clear pressure pulse during the analyzed time interval and the solar wind pressure was relatively stable.

The ion spectral energy flux density and ion bulk velocity measurements between 22:23 UT and 22:33 UT are shown in Fig. 7. It can be seen that the probes of the THEMIS fleet except THA crossed the magnetopause twice successively. At the very beginning, the THEMIS fleet was in the magnetosphere. At the first crossing, THB encountered the magnetopause at 22:24:34 UT, then THC, THD and THE crossed the magnetopause immediately after THB almost at the same time. At the second crossing, THE returned to the magnetosphere at 22:27:22 UT, then THD and THC returned to the magnetosphere about one and a half minutes after THE. At 22:32:18 UT, THB experienced its second magnetopause crossing. THA kept staying in the magnetosphere during this 10-min interval.

The right panels of Fig. 7 shows the ion bulk velocity observed by THEMIS fleet. The main difference from Event 1 is that all the THEMIS probes except THA (staying in the magnetosphere during this time interval) observed a fast anti-sunward flow. The anti-sunward flow observed by THB had a peak speed of 386 km/s at 22:25:13 UT, then the velocity began to decrease. It decreased to nearly zero when THE returned to the magnetosphere at 22:27:22 UT. Between 22:25:03 UT and 22:27:22 UT, THB, THC&D and THE were all in the magnetosheath.

The magnetic field strength curves for all probes during the same time interval are plotted in Fig. 8. Similar

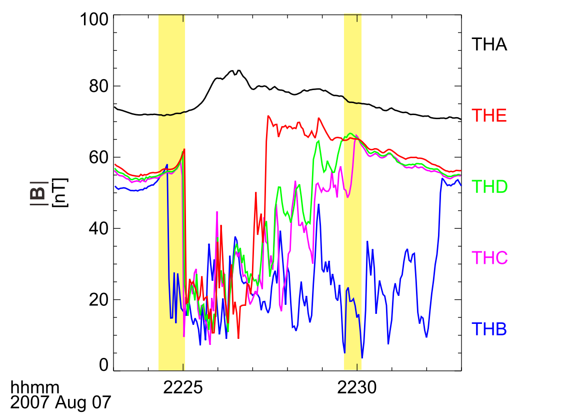

Fig. 8 The magnetic field strengths observed by the THEMIS fleet between 22:23 UT and 22:33 UT on 07 August 2007. The discussed FMGDRs are marked by yellow bars

to Event 1, there are many intersections between different curves. The main difference between the two events is that the magnetic field strength observed by THA was always the largest among the observations of five probes in Event 2.

Similar to Fig. 4, Fig. 9 shows the calculated tangential planes of the magnetopause crossing encountered by the THEMIS probes (short colored lines), and the observed flow vectors (black arrows) projected to the X–Y plane. For comparison, the nominal magnetopause planes are also plotted in the large red curves. Figures 9a–d show the snapshots when THB, THC, THD and THE crossed the magnetopause at the first time for this event. It can be seen that the tangential plane moved inward at a large angle relative to the nominal magnetopause plane and the bulk velocity of ions was nearly parallel to the tangential plane. Figures 9e–h are the snap-

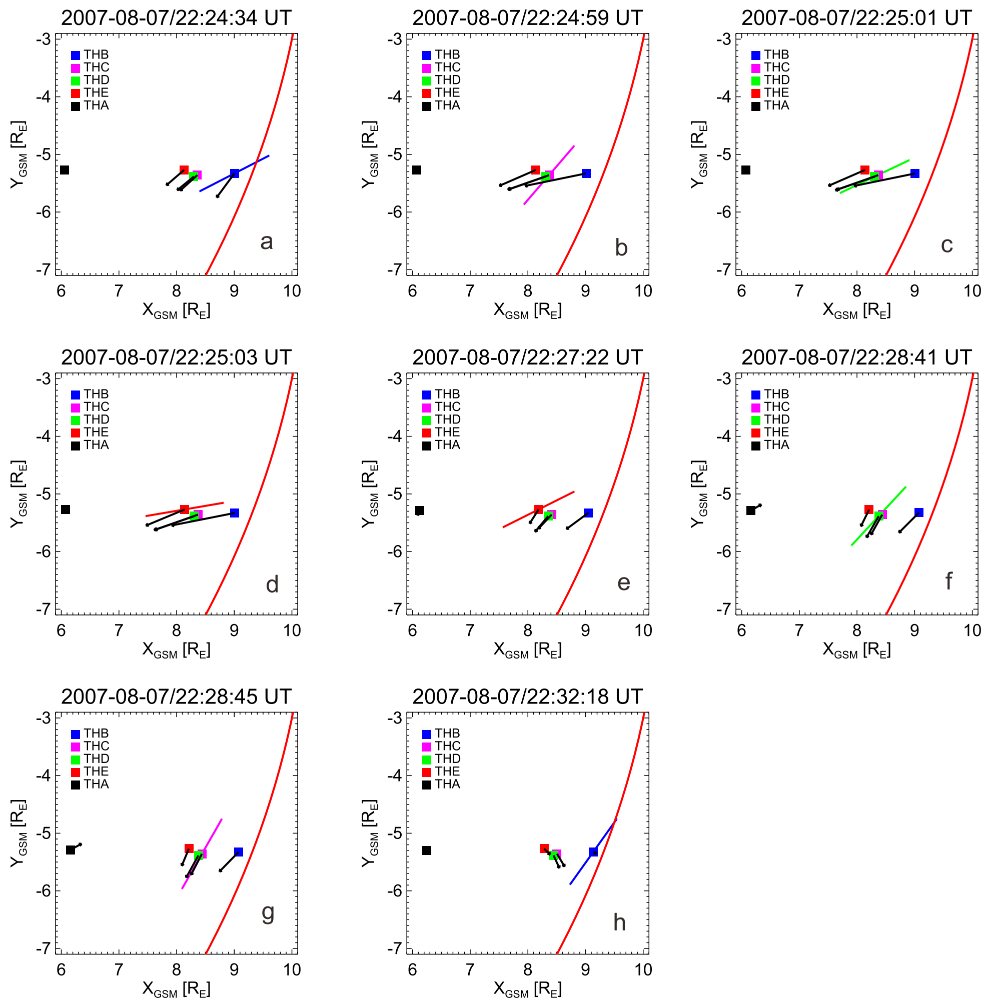

Fig. 9 Comparisons of the tangential planes calculated by MVA (short colored lines) and the nominal magnetopause planse calculated by Shue et al. (1998) (large red curve). The black arrows are the ion velocity observed by the THEMIS probes

shots when THE, THD, THC and THB crossed the magnetopause for the second time. The tangential plane in Fig. 9e remained the same angle with the nominal magnetopause plane. It was roughly parallel to the nominal magnetopause plane in Figs. 9f–h. The bulk velocity of ions observed at the second crossing (except Fig. 9h) are roughly parallel to the tangential plane, but it is much smaller than that observed at the first crossing.

All observations of the variations in the calculated magnetopause tangential planes and ion flows can be explained by an encountered of an evolving local indentation driven by a fast magnetosheath flow observed by THB, as shown in Figs. 9b–d. Figure 10 shows the schematic pictures for the fast magnetosheath flow and distorted magnetopause evolving over time. In Fig. 10a, the fast anti-sunward magnetosheath flows impacted the magnetopause, causing the generation of the local magnetopause indentation. THB was located at the upper part of the indentation, so the tangential plane leaned to the right relative to the nominal magnetopause plane. The velocity of the anti-sunward flow continued to increase and compressed the magnetopause closer to the center of the Earth to encounter THC&D and THE (as shown in Fig. 10b) successively. At the time between

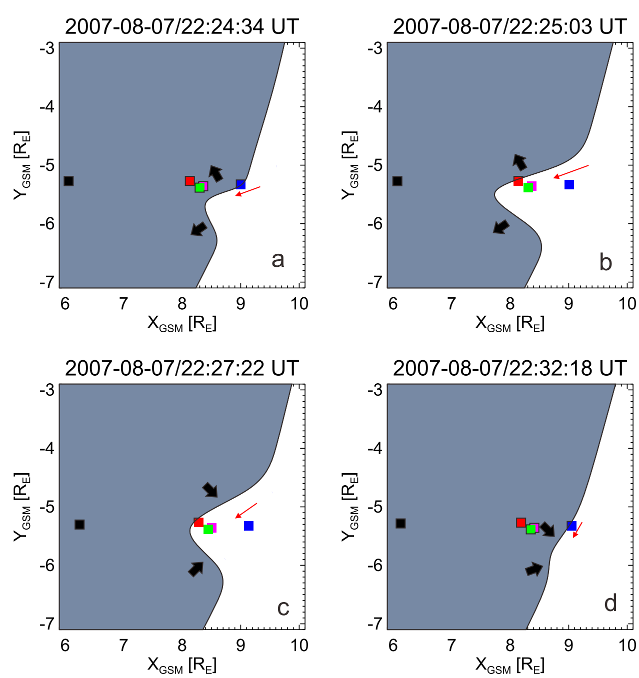

Fig. 10 Schematic pictures of the indented magnetopause. The format is the same as in Fig. 5

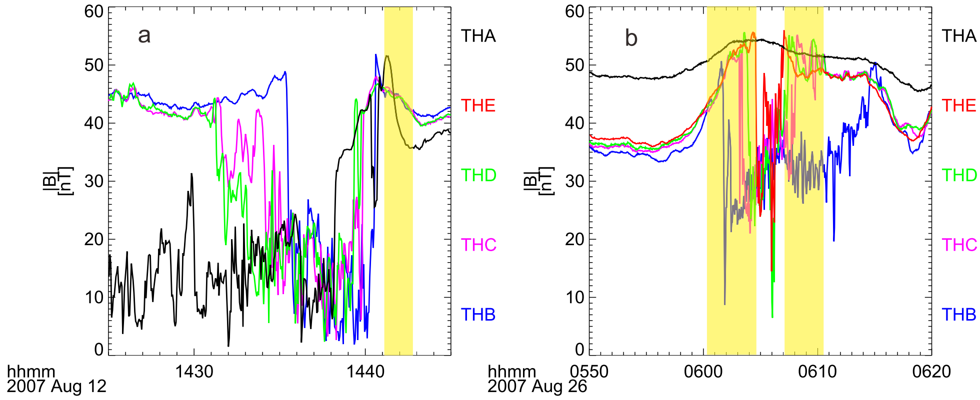

Fig. 11 (**a**, **b**) are the relative magnitude of the magnetic field strength observed by THEMIS fleet in the events reported by Shue et al. (2009) and Tkachenko et al. (2011), respectively. FMGDRs are marked by yellow bars

22:25:03 UT (Fig. 10b) and 22:27:22 UT (Fig. 10c), the anti-sunward flow in the magnetosheath became weaker, indicating that the indentation was recovering. In Fig. 10c, the indentation became shallower and smoother and it disappeared at 22:32:18 UT (see Fig. 10d). Thus the tangential planes observed by THC, THD and THB at the second crossing were almost parallel to the nominal magnetopause plane.

3 Discussion

In the literature, there are few analyses on the observations of the magnetopause indentation phenomena. Here we report two typical events and find the simultaneous occurrence of the indentation of the magnetopause and FMGDR. On the other hand, as shown in the right panel of Figs. 1 and 6, there are no clear solar wind pressure pulse in these two typical events. We also check the observation of GOES 11 (15:50 MLT) for the first case and GOES 11 (13:30 MLT) for the second case, and no magnetic pulse was found. So we consider that the FMGDR can not be caused by the global compression and it may be caused by the magnetopause local indentation.

The locally indented magnetopause was also reported by Shue et al. (2009) and Tkachenko et al. (2011), but they did not show the observational features of magnetic fields adjacent to the indented magnetopause. Here we reinvestigate their events from a perspective of magnetic field variations affected by an indented magnetopause. Figure 11a presents the magnetic field observation corresponding to the event shown in Fig. 2 in Shue et al. (2009). For this case, the magnetopause was not indented at the first crossing and the magnetic gradient pointed inward. But at the second crossing, the magnetopause was distorted by a small-scale fast anti-sunward magnetosheath flow and rebounded subsequently. During the second crossing, the FMGDR can be seen as marked by yellow bar. Figure 11b presents magnetic field observations corresponding to the event shown in Fig. 5 in Tkachenko et al. (2011). For this case, the THEMIS fleet encountered an indentation moving to the dawn flank and the four probes (except THA) crossed the magnetopause twice successively. The observed magnetic field from outer probes exceeds those from inner probes, which is similar to those shown in Figs. 3 and 8. In summary, in the events including those analyzed in this paper as well as those reported by Shue et al. (2009) and Tkachenko et al. (2011), when the THEMIS probes crossed the indented magnetopause, they all observed FMGDR phenomena.

In fact whether FMGDR can be observed depends on the relative position of the THEMIS fleet and the indented magnetopause. At the first crossing of Event 2, the magnetic field strength observed by THB, THC, THD and THE were enhanced, but that observed by THA remained unchanged most likely because THA was too far away from the indented magnetopause. THA was out of the influence area of the indented magnetopause. As the indentation became deeper, the magnetic field strength observed by THA began to increase. On the other hand, It can be deduced that the magnetic field strength at the edge of the indentation is the largest as it is usually most compressed at the edge. If the THEMIS fleet was configurated along the edge of the indentation, FMGDR may not be observed. In addition, the magnetic field strength observed at the second crossing was lower than that observed at the first crossing in Event 1. It is most likely related to the asymmetry of the indentation.

As mentioned in Sect. 1, there are many sources of the magnetopause waves or local indentations. In these two events, the indentations may be caused by the anomalous fast anti-sunward magnetosheath flow as shown in Figs. 2 and 7. The source of the fast anti-sunward magnetosheath flow and how it generated the magnetopause deformation are out of the scope of this paper.

4 Summary

The large-scale magnetopause has been studied comprehensively over recent decades. Due to lack of simultaneous observations from multiple spacecrafts before, the small structures of the magnetopause have been rarely reported and analyzed. Here we report two typical events of the indented magnetopause crossing observed by THEMIS fleet. FMGDR is observed in each crossing. We also reexamined the magnetic field distribution near the magnetopause when THEMIS encountered the magnetopause indentations reported by Shue et al. (2009) and Tkachenko et al. (2011). The same phenomena were found in their events. These observations show that FMGDR can be generated adjacent to the indented magnetopause. Our paper gives a possible explanation to the observed FMGDR.

Acknowledgements We acknowledge NASA contract NAS5-02099 and V. Angelopoulos for use of data from the THEMIS Mission. Specifically, we ackonwledge C.W. Carlson and J.P. McFadden for use of ESA data, K.H. Glassmeier, U. Auster and W. Baumjohann for the use of FGM data provided under the lead of the Technical University of Braunschweig and with financial support through the German Ministry for Economy and Technology and the German Center for Aviation and Space (DLR) under contract 50 OC 0302. The THEMIS data were downloaded from the website http://themis.ssl.berkeley.edu/data/themis/. This work is jointly supported by the National Natural Science Foundation of China (41731067, 41531073), the Specialized Research Fund for State Key Laboratories of China, 973 program (2012CB825601) and Shenzhen Technology Project JCYJ20170307150645407.

References

Angelopoulos, V.: Space Sci. Rev. **141**(1), 5 (2008)
Auster, H.U., Glassmeier, K.H., Magnes, W., Aydogar, O., Baumjohann, W., Constantinescu, D., Fischer, D., Fornacon, K.H., Georgescu, E., Harvey, P., Hillenmaier, O., Kroth, R., Ludlam, M., Narita, Y., Nakamura, R., Okrafka, K., Plaschke, F., Richter, I., Schwarzl, H., Stoll, B., Valavanoglou, A., Wiedemann, M.: Space Sci. Rev. **141**(1-4), 235 (2008)
Chapman, S., Ferraro, V.C.A.: J. Geophys. Res. **38**(2), 79 (1930)
Dmitriev, A.V., Suvorova, A.V.: J. Geophys. Res. Space Phys. **117**, 08217 (2012)
Fairfield, D.H.: J. Geophys. Res. **76**(28), 6700 (1971)
Fairfield, D.H., Baumjohann, W., Paschmann, G., Luhr, H., Sibeck, D.G.: J. Geophys. Res. Space Phys. **95**(A4), 3773 (1990)
Fujita, S., Glassmeier, K.H., Kamide, K.: J. Geophys. Res. Space Phys. **101**(A12), 27317 (1996)
Ganushkina, N.Y., Liemohn, M.W., Dubyagin, S., Daglis, I.A., Dandouras, I., De Zeeuw, D.L., Ebihara, Y., Ilie, R., Katus, R., Kubyshkina, M., Milan, S.E., Ohtani, S., Ostgaard, N., Reistad, J.P., Tenfjord, P., Toffoletto, F., Zaharia, S., Amariutei, O.: Ann. Geophys. **33**(11), 1369 (2015)
Glassmeier, K.H., Heppner, C.: J. Geophys. Res. Space Phys. **97**(A4), 3977 (1992)
Han, D.: Sci. China Earth Sci. **62**, 1 (2019). https://doi.org/10.1007/s11430-019-9358-8
Han, D.-S., Chen, X.-C., Liu, J.-J., Qiu, Q., Keika, K., Hu, Z.-J., Liu, J.-M., Hu, H.-Q., Yang, H.-G.: J. Geophys. Res. Space Phys. **120**(9), 7447 (2015)
Han, D.S., Nishimura, Y., Lyons, L.R., Hu, H.Q., Yang, H.G.: Geophys. Res. Lett. **43**(5), 1819 (2016)
Han, D.S., Hietala, H., Chen, X.C., Nishimura, Y., Lyons, L.R., Liu, J.J., Hu, H.Q., Yang, H.G.: J. Geophys. Res. Space Phys. **122**(2), 1853 (2017)
Han, D.-S., Liu, J.J., Chen, X.C., Xu, T., Li, B., Hu, Z.J., Hu, H.Q., Yang, H.G., Fuselier, S.A., Pollock, C.J.: J. Geophys. Res. Space Phys. **123**(4), 2658 (2018)
Han, D., Xu, T., Jin, Y., Oksavik, K., Chen, X., Liu, J., Zhang, Q., Baddeley, L., Herlingshaw, K.: Geophys. Res. Lett. **46**(13), 7113 (2019)
McFadden, J.P., Carlson, C.W., Larson, D., Ludlam, M., Abiad, R., Elliott, B., Turin, P., Marckwordt, M., Angelopoulos, V.: Space Sci. Rev. **141**(1-4), 277 (2008)
Petrinec, S.P., Song, P., Russell, C.T.: J. Geophys. Res. Space Phys. **96**(A5), 7893 (1991)
Plaschke, F., Angelopoulos, V., Glassmeier, K.H.: J. Geophys. Res. Space Phys. **118**(4), 1483 (2013)
Shue, J.H., Song, P., Russell, C.T., Steinberg, J.T., Chao, J.K., Zastenker, G., Vaisberg, O.L., Kokubun, S., Singer, H.J., Detman, T.R., Kawano, H.: J. Geophys. Res. Space Phys. **103**(A8), 17691 (1998)
Shue, J.H., Chao, J.K., Song, P., McFadden, J.P., Suvorova, A., Angelopoulos, V., Glassmeier, K.H., Plaschke, F.: Geophys. Res. Lett. **36**, 18112 (2009)
Song, P., DeZeeuw, D.L., Gombosi, T.I., Groth, C.P.T., Powell, K.G.: J. Geophys. Res. Space Phys. **104**(A12), 28361 (1999)
Sonnerup, B.U.., Scheible, M.: ISSI Sci. Rep. Ser. **1**, 185 (1998)
Spreiter, J.R., Summers, A.L., Alksne, A.Y.: Planet. Space Sci. **14**(3), 223 (1966)
Tkachenko, O., Safrankova, J., Nemecek, Z., Sibeck, D.G.: Ann. Geophys. **29**(4), 687 (2011)
Tsyganenko, N.A.: Planet. Space Sci. **37**, 5 (1989)
Tsyganenko, N.A.: In: International Conference on Substorms, vol. 389, p. 181 (1996)